JACS
JOURNAL OF THE AMERICAN CHEMICAL SOCIETY

Communication

pubs.acs.org/JACS

Luminescent Covalent Organic Frameworks Containing a Homogeneous and Heterogeneous Distribution of Dehydrobenzoannulene Vertex Units

Jonathan W. Crowe, Luke A. Baldwin, and Psaras L. McGrier*

Department of Chemistry & Biochemistry, The Ohio State University, Columbus, Ohio 43210, United States

Supporting Information

ABSTRACT: Finding new ways to construct crystalline multiple-component covalent organic frameworks (COFs) has become an important focus. Herein we report the synthesis of three novel COFs containing a homogeneous and heterogeneous distribution of π-conjugated dehydrobenzoannulene (DBA) vertex units. The COFs were synthesized by reacting different ratios of C_3-symmetric DBA catechol monomers with C_2-symmetric pyrene-2,7-diboronic acid (PDBA) to yield three COFs, Py-DBA-COF 1, Py-DBA-COF 2, and Py-MV-DBA-COF. All three materials are highly crystalline and display unique luminescent properties in the solid state.

Covalent organic frameworks (COFs)[1−3] are an advanced class of porous crystalline materials that enable the specific inclusion of various π-conjugated units into highly ordered periodic arrays. This feature allows the properties of the materials to be tailored for applications pertaining to gas storage,[4,5] catalysis,[6,7] separations,[8] energy storage,[9] optoelectronics,[10−14] and proton conduction.[15,16] Since COFs are typically constructed through a reversible dynamic nucleation−elongation process,[17] the surface area, pore size, and structural topology of the materials can be conveniently modified by careful selection of the molecular building blocks. Although many COFs possessing high surface areas and uniform pore channels have been reported, there has been an increased effort to create other COF materials that contain heterogeneous pore channels[18−22] or different types of π-conjugated monomers by utilizing a mixed-linker strategy.[23] Such explorations are believed to be important not only to increase the structural diversity of COFs but also to provide access to ordered polymeric materials with unique separation, optoelectronic, and gas adsorption properties.

Recently, Zhao and co-workers have shown[24] that by the use of an orthogonal reaction strategy in which two different functional groups are attached to one monomer, two different types of covalent bonds and vertex units can be incorporated into one COF structure. Intrigued by this work, we were curious to determine whether a mixed-vertex strategy could be used to create a COF material containing an assortment of heterogeneous pore sizes using only one type of covalent bond. We hypothesized that mixing C_3-symmetric triangular-shaped monomers of different pore sizes in a 1:1 ratio with a C_2-symmetric ditopic linker could yield a hexagonal-shaped COF structure with a heterogeneous distribution of vertex units (Scheme 1c). To test this strategy, we decided to use C_3-symmetric π-conjugated dehydrobenzoannulenes (DBAs) and

Scheme 1. Design of DBA-COFs Containing a Mixture of Hexagonal and (A) Small Triangular, (B) Large Triangular, or (C) Small and Large Triangular Vertices

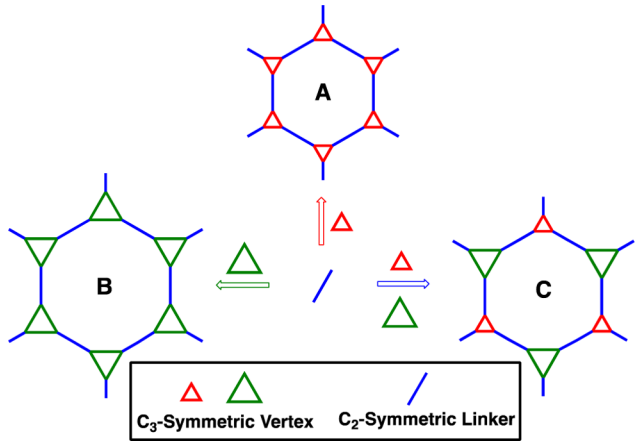

C_2-symmetric pyrene-2,7-diboronic acid (PDBA) as our vertex and ditopic linker molecular building blocks. DBAs are planar carbon-rich macrocycles that contain triangular pores and exhibit unique optoelectronic properties.[25] We[26] and others[27] have shown that DBA[12][28] and DBA[18] monomers can be utilized to create highly luminescent porous materials. However, the incorporation of both DBA monomers into one two-dimensional (2D) COF has yet to be reported.

To begin our study, we first reacted DBA[12] with PDBA under solvothermal conditions in a 2:1 (v/v) 1,4-dioxane and mesitylene mixture at 105 °C for 3 days to produce Py-DBA-COF 1 (Scheme 2). Py-DBA-COF 2 and Py-MV-DBA-COF were constructed under similar reaction conditions with the exception of utilizing a 2:1 (v/v) 3-pentanone and mesitylene solvent mixture on account of the limited solubility of DBA[18] in dioxane. It should be noted that the ideal reaction conditions described above were achieved after carefully screening different monomer and solvent ratios (see pp S4−S5 in the Supporting Information (SI) for details). All three COFs were obtained by transferring and suspending the remaining solids in acetonitrile or tetrahydrofuran.

Received: June 24, 2016
Published: August 4, 2016

DOI: 10.1021/jacs.6b06546
J. Am. Chem. Soc. 2016, 138, 10120−10123

Scheme 2. Synthesis of DBA-COFs

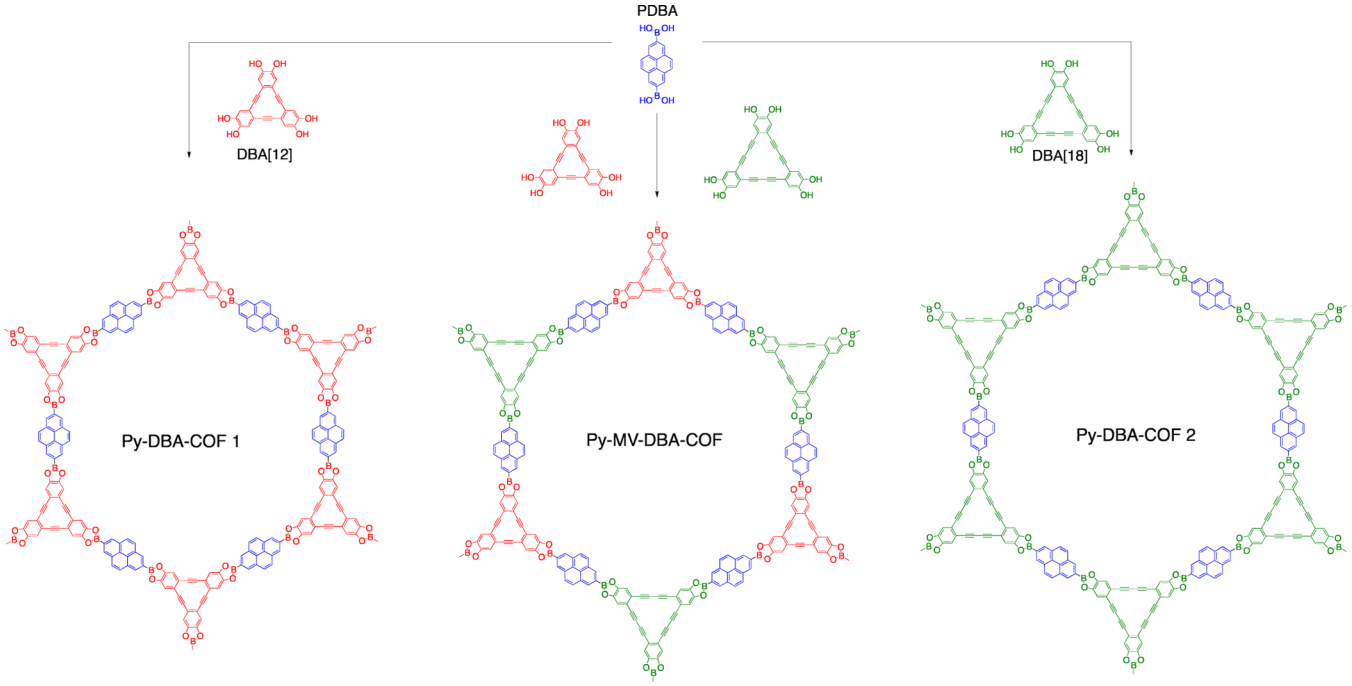

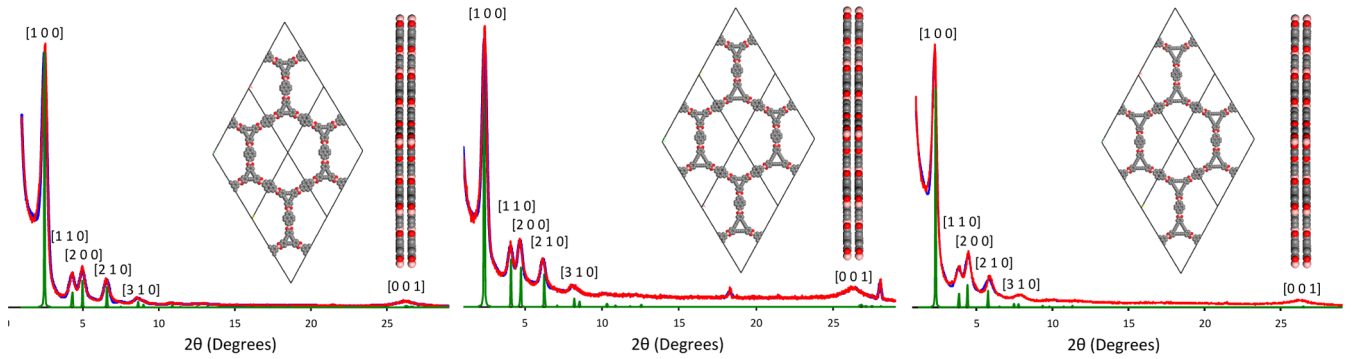

Figure 1. Indexed experimental (red) and Pawley-refined (blue) PXRD profiles of Py-DBA-COF 1 (left), Py-MV-DBA-COF (middle), and Py-DBA-COF 2 (right) overlaid with the bnn-simulated patterns (green). The extra reflection peaks at 18° and 28° for Py-MV-DBA-COF are from H_3BO_3, a decomposition product formed in the presence of moisture.[12]

The formation of the boronate ester (B−O) linkages for Py-DBA-COF 1, Py-DBA-COF 2, and Py-MV-DBA-COF were confirmed by Fourier transform infrared (FT-IR) spectroscopy, exhibiting stretching modes at 1332, 1329, and 1328 cm^{-1}, respectively (Figures S1−S3 in the SI). Thermogravimetric analysis (TGA) revealed that all three DBA-COFs displayed excellent thermal stability, maintaining more than 96% of their weight up 400 °C (Figures S11−S13). The solid-state ^{13}C cross-polarization magic-angle spinning (CP-MAS) NMR spectra of Py-DBA-COF 1 and Py-DBA-COF 2 revealed the characteristic resonances of the alkynyl units at ∼92.6 and 78.2 ppm, respectively (Figures S17 and S18). In comparison, Py-MV-DBA-COF exhibited two broad resonances at ∼91.7 and 78.7 ppm, which confirmed the incorporation of both DBA[12] and DBA[18] monomers into one COF structure (Figure S19). Scanning electron microscopy (SEM) images of Py-DBA-COF 1 revealed the existence of ball-shaped and elongated needle-shaped crystallites (Figure S20), whereas Py-DBA-COF 2 and Py-MV-DBA-COF displayed a cauliflower-like morphology (Figures S21 and S22).

Figure 1 shows the experimental and refined powder X-ray diffraction (PXRD) profiles for Py-DBA-COF 1, Py-DBA-COF 2, and Py-MV-DBA-COF, which were indexed utilizing a primitive hexagonal unit cell. Py-DBA-COF 1 displayed strong peaks at 2.51, 4.33, 4.98, 6.55, 8.52, and 25.9°, corresponding to the (100), (110), (200) (210), (310), and (001) planes, respectively. The PXRD profile for Py-DBA-COF 2 was slightly shifted to lower angles, exhibiting peaks at 2.25, 3.87, 4,45, 5.83, 7.67, and 26.1, which also correspond to the (100), (110), (200) (210), (310), and (001) planes, respectively. Simulated PXRD patterns of Py-DBA-COF 1 and Py-DBA-COF 2 were produced using an eclipsed bnn (*P6/mmm*) hexagonal unit cell.[29] Pawley refinement of the experimental data for Py-DBA-COF 1 provided unit cell parameters of $a = b = 41.014$ Å and $c = 3.4$ Å (residuals $R_p = 6.06$, $R_{wp} = 7.73$), whereas Py-DBA-COF 2 provided unit cell parameters of $a = 48.622$ Å, $b = 48.834$ Å, and $c = 3.39$ Å (residuals $R_p = 5.43$, $R_{wp} = 6.76$). The simulated spectra were in good agreement with the experimental values for both COFs.

DOI: 10.1021/jacs.6b06546
J. Am. Chem. Soc. 2016, 138, 10120−10123

In comparison, Py-MV-DBA-COF unveiled peaks at 2.37, 4.06, 4.66, 6.11, 7.83, and 25.9°, corresponding to the (100), (110), (200) (210), (310), and (001) planes, respectively. Pawley refinement of the experimental data provided unit cell parameters of a = 43.042 Å, b = 43.223 Å, and c = 3.33 Å (residuals R_p= 6.06, R_{wp}= 7.73). These values were also in good agreement with the bnn net simulated data. In order to confirm the ratio of DBA[12] and DBA[18] monomers, we performed a ^{1}H NMR experiment in which 3 mg of Py-MV-DBA-COF was hydrolyzed in dimethyl sulfoxide-d_6 by adding 50 μL of 1 M HCl. Interestingly, the ^{1}H NMR spectrum revealed a 1:1.12 molar ratio of DBA[18] and DBA[12], respectively (Figure S33). We believe that the two DBA vertices for Py-MV-DBA-COF are incorporated in an alternating manner throughout the COF (Scheme 2). In addition, we also considered staggered gra ($P6_3/mmm$) packing conformations for all of the DBA-COFs. However, the experimental data did not match the simulated profiles (Figures S6, S8, and S10).

The porosity of each DBA-COF was evaluated by measuring nitrogen gas adsorption/desorption isotherms at 77 K (Figure 2). Py-DBA-COF 1 and Py-DBA-COF 2 both exhibited type-IV

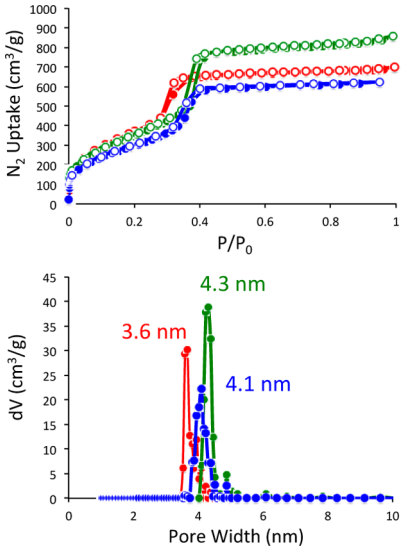

Figure 2. Nitrogen adsorption/desorption isotherms (top) and NLDFT pore size distributions (bottom) for Py-DBA-COF 1 (red), Py-DBA-COF 2 (green), and Py-MV-DBA-COF (blue) measured at 77 K.

isotherms, which are indicative of mesoporous materials. Py-DBA-COF 1 displayed a sharp uptake at low relative pressure (P/P_0 < 0.01) followed by a sharp step between P/P_0 = 0.04 and 0.32, while Py-DBA-COF 2 exhibited similar uptake characteristics with the exception of revealing a step between P/P_0 = 0.05 and 0.37. The Brunauer–Emmett–Teller (BET) model was applied to the data for Py-DBA-COF 1 and Py-DBA-COF 2 over the low-pressure region of the isotherm (0.04/0.05 < P/P_0 < 0.25) to provide surface areas of 1392 and 1354 m^2 g^{-1}, respectively. The total pore volumes of Py-DBA-COF 1 and Py-DBA-COF 2, calculated at P/P_0 = 0.994 and 0.991, respectively, both were 1.21 cm^3/g. In comparison, Py-MV-DBA-COF also displayed a type-IV isotherm, and applying the BET model over the low-pressure region (0.06 < P/P_0 < 0.26) afforded a surface area of 1134 m^2 g^{-1}. The total pore volume evaluated at P/P_0 = 0.949 was 1.06 cm^3/g. The pore size distributions for Py-DBA-COF 1, Py-DBA-COF 2, and Py-MV-DBA-COF were estimated using nonlocal density functional theory (NLDFT), which provided values of 3.6, 4.3, and 4.1 nm, respectively. The experimental values for Py-DBA-COF 1, Py-DBA-COF 2, and Py-MV-DBA-COF were very close to their theoretical pore sizes of 3.8, 4.3, and 4.1 nm, respectively, which were estimated using the bnn models. It should be noted that Py-MV-DBA-COF contains the largest pore size reported for a COF containing mixed vertices.

In addition, all three DBA-COFs are highly luminescent in the solid state (Figure 3). Upon excitation of the DBA[18]

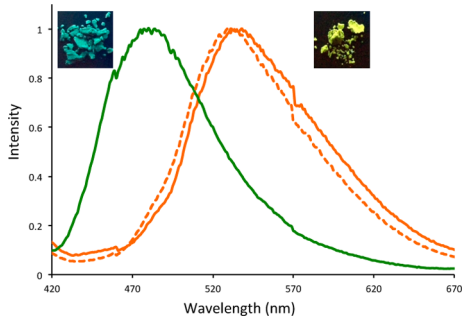

Figure 3. Normalized emission spectra and photographs of Py-DBA-COF 1 (orange, λ_{exc} = 350 nm), Py-DBA-COF 2 (green, λ_{exc}= 365 nm), and Py-MV-DBA-COF (oranged dashed, λ_{exc} = 350 nm). The photographs of the fluorescent solids were taken using a hand-held UV-lamp at 365 nm.

units at 365 nm, the solid-state powder of Py-DBA-COF 2 exhibited a blue-greenish luminescent color with a λ_{max} of 483 nm. In contrast, the emission wavelengths of Py-DBA-COF 1 and Py-MV-DBA-COF are red-shifted by ~47 nm, providing a λ_{max} of 530 and 528 nm (λ_{exc} = 350 nm), respectively. The powders of both COFs displayed yellow luminescence under UV radiation. The large bathochromic shifts for these two COFs is likely due to the fact that the lowest-energy transitions of DBA[12]-based materials are symmetry-forbidden in the ground state compared with DBA[18]-based materials (Figures S29 and S30).[30,31] Interestingly, the presence of the DBA[12] units rather than the DBA[18] units appears to dominate the excited-state properties of Py-MV-DBA-COF. UV–vis diffuse-reflectance spectra indicate that all three DBA-COFs exhibit broad absorption bands ranging from 300 to 420 nm (Figures S23, S25, and S27).

In summary, we have demonstrated that DBA monomer units can be used to construct crystalline luminescent COFs with a homogeneous and heterogeneous distribution of vertex components. We believe that the mixed-vertex approach described herein is a complement to the mixed-linker strategy and that the combination of the two approaches could undoubtedly lead to the synthesis of other highly diverse multicomponent COF systems. Such investigations could be beneficial for constructing crystalline porous organic materials with unique optoelectronic, separation, or gas adsorption properties.

■ ASSOCIATED CONTENT

Supporting Information

The Supporting Information is available free of charge on the ACS Publications website at DOI: 10.1021/jacs.6b06546.

Synthetic procedures and FT-IR, solid-state ^{13}C NMR, TGA, PXRD, and SEM data (PDF)

DOI: 10.1021/jacs.6b06546
J. Am. Chem. Soc. 2016, 138, 10120–10123

AUTHOR INFORMATION

Corresponding Author

*mcgrier.1@osu.edu

Notes

The authors declare no competing financial interest.

ACKNOWLEDGMENTS

P.L.M. acknowledges the National Science Foundation and Georgia Tech Facilitating Academic Careers in Engineering and Science (GT-FACES) for a Career Initiation Grant and funding from The American Chemical Society Petroleum Research Fund (55562-DNI7) and The Ohio State University. We thank Prof. Joshua Goldberger for helpful discussions.

REFERENCES

(1) Côté, A. P.; Benin, A. I.; Ockwig, N. W.; O'Keeffe, M.; Matzger, A. J.; Yaghi, O. M. *Science* **2005**, *310*, 1166−1170.

(2) Tilford, R. W.; Gemmill, W. R.; zur Loye, H.-C.; Lavigne, J. J. *Chem. Mater.* **2006**, *18*, 5296−5301.

(3) Feng, X.; Ding, X.; Jiang, D. *Chem. Soc. Rev.* **2012**, *41*, 6010−6022.

(4) Furukawa, H.; Yaghi, O. M. *J. Am. Chem. Soc.* **2009**, *131*, 8875−8883.

(5) Zeng, Y.; Zou, R.; Zhao, Y. *Adv. Mater.* **2016**, *28*, 2855−2873.

(6) Ding, S.-Y.; Gao, J.; Wang, Q.; Zhang, Y.; Song, W.-G.; Su, C.-Y.; Wang, W. *J. Am. Chem. Soc.* **2011**, *133*, 19816−19822.

(7) Fang, Q.; Gu, S.; Zheng, J.; Zhuang, Z.; Qiu, S.; Yan, Y. *Angew. Chem., Int. Ed.* **2014**, *53*, 2878−2882.

(8) Oh, H.; Kalidindi, S. B.; Um, Y.; Bureekaew, S.; Schmid, R.; Fischer, R. A.; Hirscher, M. *Angew. Chem., Int. Ed.* **2013**, *52*, 13219−13222.

(9) Deblase, C. R.; Silberstein, K. E.; Truong, T.-T.; Abruña, H. D.; Dichtel, W. *J. Am. Chem. Soc.* **2013**, *135*, 16821−16824.

(10) Wan, S.; Guo, J.; Kim, J.; Ihee, H.; Jiang, D. *Angew. Chem., Int. Ed.* **2008**, *47*, 8826−8830.

(11) Spitler, E. L.; Dichtel, W. R. *Nat. Chem.* **2010**, *2*, 672−677.

(12) Bertrand, G. H. V.; Michaelis, V. K.; Ong, T.-C.; Griffin, R. G.; Dincă, M. *Proc. Natl. Acad. Sci. U. S. A.* **2013**, *110*, 4923−4928.

(13) Dogru, M.; Handloser, M.; Auras, F.; Kunz, T.; Medina, D.; Hartschuh, A.; Knochel, P.; Bein, T. A. *Angew. Chem., Int. Ed.* **2013**, *52*, 2920−2924.

(14) Duhović, S.; Dincă, M. *Chem. Mater.* **2015**, *27*, 5487−5490.

(15) Xu, H.; Tao, S.; Jiang, D. *Nat. Mater.* **2016**, *15*, 722−726.

(16) Ma, H.; Liu, B.; Li, B.; Zhang, L.; Li, Y.-G.; Tan, H.-Q.; Zang, H.-Y.; Zhu, G. *J. Am. Chem. Soc.* **2016**, *138*, 5897−5903.

(17) Smith, B. J.; Dichtel, W. R. *J. Am. Chem. Soc.* **2014**, *136*, 8783−8789.

(18) Zhou, T.-Y.; Xu, S.-Q.; Wen, Q.; Pang, Z.-F.; Zhao, X. *J. Am. Chem. Soc.* **2014**, *136*, 15885−15888.

(19) Zhu, Y.; Wan, S.; Jin, Y.; Zhang, W. *J. Am. Chem. Soc.* **2015**, *137*, 13772−13775.

(20) Yang, H.; Du, Y.; Wan, S.; Trahan, G. D.; Jin, Y.; Zhang, W. *Chem. Sci.* **2015**, *6*, 4049−4053.

(21) Xu, S. Q.; Zhan, T.-G.; Wen, Q.; Pang, Z.-F.; Zhao, X. *ACS Macro Lett.* **2016**, *5*, 99−102.

(22) Dalapati, S.; Jin, E.; Addicoat, M.; Heine, T.; Jiang, D. *J. Am. Chem. Soc.* **2016**, *138*, 5797−5800.

(23) Pang, Z.-F.; Xu, S.-Q.; Zhou, T.-Y.; Liang, R.-R.; Zhan, T.-G.; Zhao, X. *J. Am. Chem. Soc.* **2016**, *138*, 4710−4713.

(24) Zeng, Y.; Zou, R.; Luo, Z.; Zhang, H.; Yao, X.; Ma, X.; Zou, R.; Zhao, Y. *J. Am. Chem. Soc.* **2015**, *137*, 1020−1023.

(25) (a) Spitler, E. L.; Johnson, C. A., II; Haley, M. M. *Chem. Rev.* **2006**, *106*, 5344−5386. (b) Haley, M. M. *Pure Appl. Chem.* **2008**, *80*, 519−532.

(26) Baldwin, L. A.; Crowe, J. W.; Shannon, M. D.; Jaroniec, C. P.; McGrier, P. L. *Chem. Mater.* **2015**, *27*, 6169−6172.

(27) Hisaki, I.; Nakagawa, S.; Ikenaka, N.; Imamura, Y.; Katouda, M.; Tashiro, M.; Tsuchida, H.; Ogoshi, T.; Sato, H.; Tohnai, N.; Miyata, M. *J. Am. Chem. Soc.* **2016**, *138*, 6617−6628.

(28) The number in brackets denotes the number of sp- and sp^2-hybridized carbon atoms within the triangular pore.

(29) Although the bnn models match, computational studies suggest that the stacking layers of most COFs are offset by ∼1.8 Å. For details, see: Koo, B. T.; Dichtel, W. R.; Clancy, P. *J. Mater. Chem.* **2012**, *22*, 17460−17469.

(30) Kamada, K.; Antonov, L.; Yamada, S.; Ohta, K.; Yoshimura, T.; Tahara, K.; Inaba, A.; Sonoda, M.; Tobe, Y. *ChemPhysChem* **2007**, *8*, 2671−2677.

(31) Anand, S.; Varnavski, O.; Marsden, J. A.; Haley, M. M.; Schlegel, H. B.; Goodson, T. *J. Phys. Chem. A* **2006**, *110*, 1305−1318.

DOI: 10.1021/jacs.6b06546
J. Am. Chem. Soc. 2016, 138, 10120−10123